

**Phonon anomalies and possible local lattice distortions in giant magnetocapacitive CdCr<sub>2</sub>S<sub>4</sub>**V. Gnezdilov,<sup>1</sup> P. Lemmens,<sup>2</sup> Yu. G. Pashkevich,<sup>3</sup> Ch. Payen,<sup>4</sup> K. Y. Choi,<sup>5</sup> J. Hemberger,<sup>6</sup> A. Loidl,<sup>6</sup> and V. Tsurkan<sup>6,7</sup><sup>1</sup>*B. I. Verkin Institute for Low Temperature Physics, NASU, 61164 Kharkov, Ukraine*<sup>2</sup>*Institute for Condensed Matter Physics, TU Braunschweig, D-38106 Braunschweig, Germany*<sup>3</sup>*A. A. Galkin Donetsk Phystech NASU, 83114 Donetsk, Ukraine*<sup>4</sup>*Institut des Matériaux Jean Rouxel, CNRS-Universite de Nantes, BP32229, 44322 Nantes cedex 3, France*<sup>5</sup>*Department of Physics, Chung-Ang University, 221 Huksuk-Dong, Dongjak-Gu, Seoul 156-756, Republic of Korea*<sup>6</sup>*Experimental Physics V, Center for Electronic Correlations and Magnetism, University of Augsburg, D-86135 Augsburg, Germany*<sup>7</sup>*Institute of Applied Physics, Academy of Sciences of Moldova, MD-2028 Chisinau, R. Moldova*

(Received 20 March 2011; published 6 July 2011)

We investigate the origin of large magnetocapacitive effects in CdCr<sub>2</sub>S<sub>4</sub> single crystals focusing on phonon anomalies in the fluctuation regime  $T < T^* = 130$  K and with the onset of ferromagnetic order  $T_c = 84.4$  K. The observation of longitudinal optical and formerly infrared active modes for  $T < T_c$  is used to propose a loss of inversion symmetry and Cr off-centering. Further anomalies in intensity, frequency, and linewidth have an onset temperature  $T^*$  that coincides with the onset of magnetocapacitive effects. The respective intensity anomalies are attributed in part to an enhanced electronic polarizability of displacements that modulate the Cr-S distance and respective hybridization. This is taken as a prerequisite to the proposed Cr off-centering. Anomalies due to the previously disregarded photodoping and resonance are analyzed comparing different excitation energies.

DOI: [10.1103/PhysRevB.84.045106](https://doi.org/10.1103/PhysRevB.84.045106)

PACS number(s): 72.80.Ga, 75.30.-m, 71.30.+h, 78.30.-j

**I. INTRODUCTION**

The coexistence and mutual coupling of magnetic and dielectric properties in solids are presently discussed from both fundamental and application points of view.<sup>1</sup> Large coupling effects have been found in different material classes, ranging from antiferromagnets (AF) with spiral ground states,<sup>1</sup> via composite or lamellar materials that provide magnetoelastic coupling at interfaces,<sup>2</sup> to lone pair systems with hybridized electronic states that gain energy by polar distortions.<sup>3</sup> The intrinsic coexistence, however, of ferromagnetic and ferroelectric order parameters is hindered by exclusive symmetry conditions and having occupied 3d electron states to provide magnetic exchange and their energetic disadvantage in polar distorted coordinations.<sup>4</sup>

Among the reported materials, the cubic thiospinel CdCr<sub>2</sub>S<sub>4</sub> ( $T_c = 84.4$  K) stands out due to its large ferromagnetic (FM) moment coexistent with a remanent dielectric polarization. Furthermore, a pronounced fluctuation regime with relaxor ferroelectric behavior<sup>5</sup> and evidence for polar nanodomains exists above  $T_c$ . This is evident from a maximum of the dielectric loss at  $T_{\max}(\omega \rightarrow 0) = T^* = 130$  K and a broadening of x-ray peaks.<sup>6</sup> Most unusual in these observations is the  $Fd\bar{3}m$  space group symmetry of the paramagnetic phase. This group symmetry strictly forbids the existence of a ferroelectric order parameter. Therefore, mesoscopic or microscopic variations of the electronic state which create local distortions may play an important role for the relaxation effects and magnetocapacitive effects.<sup>7</sup> In its turn magnetocapacity above  $T_c$  might arise due to magnetoelectric coupling between magnetic moment fluctuations and local distortions. Similar to manganites, the cross susceptibilities could be magnified by microscopic phase separation.<sup>8,9</sup> As suggested by Hemberger *et al.*<sup>5</sup> off-centering of Cr ions in CdCr<sub>2</sub>S<sub>4</sub> could serve as an intrinsic mechanism for this effect. Also in far-infrared studies<sup>10</sup> of CdCr<sub>2</sub>S<sub>4</sub>, significant effects are detected in the temperature dependence

of the plasma frequencies, indicating changes in the nature of the bonds and significant charge redistribution.

On the other hand, there is evidence for a nonintrinsic nature of some dielectric anomalies (see discussion in Refs. 9 and 10). Problems may arise due to nonstoichiometry, finite conductivity, and possible internal interfaces of some samples that impede a proper dielectric characterization. Nevertheless, record values of magnetocapacitive effects with an increase of the dielectric constant  $\epsilon'$  of up to a factor of 30 in a magnetic field of 10 T are reported.<sup>7</sup> Due to the lack of microscopic information, understanding of the underlying physics is rather limited and requires further spectroscopic investigation as well as high-quality samples prepared by different growth methods.

In the present paper, pronounced anomalies of the phonon systems based on Raman light scattering (RS) on single crystals of CdCr<sub>2</sub>S<sub>4</sub> are reported. Following intense study and optimization of preparation parameters, we use CdCr<sub>2</sub>S<sub>4</sub> single crystals grown by Br transport. These crystals are expected to be free from transport agent contaminations. However, they are smaller in size than samples from Cl transport. Based on the observation of longitudinal polar phonons in our Raman spectra, we suggest a noncentrosymmetric  $F\bar{4}3m$  crystal structure at low temperatures ( $T < T_c$ ), clearing up a longstanding dispute<sup>5,11</sup> on a possible Cr off-centering and loss of inversion symmetry. Polar phonons that modulate the Cr-S distances show large intensity gains in magnetically ordered phase that point to an intrinsic magnetoelectric coupling effect of the magnetic degrees of freedom and local polarizations. Furthermore, we demonstrate that the onset of these anomalies exists already in the fluctuation region for  $T_c < T < T^*$ .

**II. EXPERIMENT**

RS experiments were performed on as-grown, shiny [111] surfaces of CdCr<sub>2</sub>S<sub>4</sub> single crystals prepared from a Br transport reaction. Spectra of the scattered radiation were

collected by a Dilor-XY triple spectrometer and recorded by a nitrogen-cooled, charge-coupled device detector. We used the excitation wavelengths  $\lambda = 632.8$  nm of a HeNe laser,  $\lambda = 488$  nm of an Ar/Kr ion laser, and  $\lambda = 532.1$  nm of a solid-state laser with a power level  $P < 6$  mW, i.e. a factor 15 less than in previous studies.<sup>12–14</sup> In our experiments, we used parallel (*XX*) and crossed (*XY*) light polarizations. Temperature dependencies were investigated using a variable temperature closed-cycle cryostat (Oxford/Cryomech Optistat, RT-2.8 K) and a continuous helium flow optical cryostat (Cryovac, RT-3K).

### III. RESULTS AND DISCUSSION

Earlier RS experiments<sup>12–14</sup> showed agreement with factor group calculations for the room temperature structure  $Fd\bar{3}m$  which is cubic and inversion symmetric.<sup>15</sup> The decomposition of the Raman-active symmetry components leads to  $\Gamma = A_{1g}(394) + E_{1g}(257) + 3T_{2g}(99, 280, 352)$  with the calculated phonon frequencies given in brackets ( $\text{cm}^{-1}$ ).<sup>15,16</sup>

In Fig. 1 Raman spectra of  $\text{CdCr}_2\text{S}_4$  measured in two scattering geometries are presented. At room temperature, very sharp maxima are observed, thus proving the high quality of the used single crystals. Also the background level of the spectra is uniform and flat. Samples that are defect rich or nonstoichiometric show broad maxima due to fluorescence

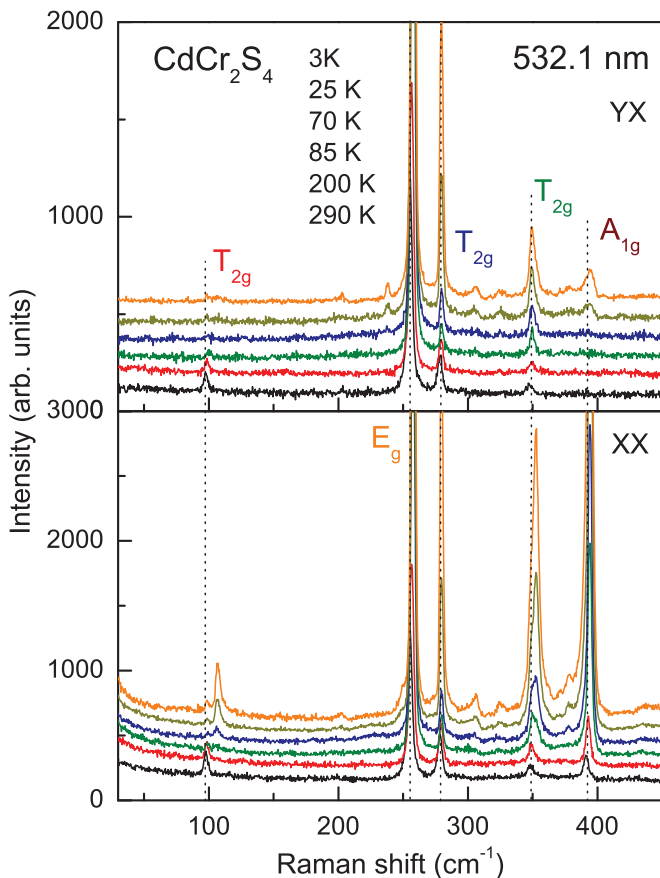


FIG. 1. (Color online) RS spectra of  $\text{CdCr}_2\text{S}_4$  as a function of temperature taken with  $\lambda = 532.1$  nm. The curves are shifted for clarity. The phonon lines are marked by dashed lines and assigned according to the high-temperature structure (Ref. 15).

effects. The number and frequencies of the excitations are in detailed agreement with lattice calculations<sup>16</sup> based on the space group  $Fd\bar{3}m$ . The modes are marked by dashed lines and with the respective symmetry representation. The  $A_{1g}$  phonon line is observed only in *XX* scattering geometry without any leakage in the *XY* scattering geometry. With decreasing temperature, several anomalies develop. Most spectacular is the appearance of a new mode at  $106 \text{ cm}^{-1}$ , i.e.  $8 \text{ cm}^{-1}$  higher than the lowest frequency mode at  $98 \text{ cm}^{-1}$ . At the same time, the high-frequency phonons with  $\Delta\omega > 250 \text{ cm}^{-1}$  show different intensity versus temperature dependencies for different incoming photon energies. While all four phonon modes show an enormous gain in intensity with the excitation wavelengths  $\lambda = 532.1$  nm, only two phonon modes with  $\Delta\omega > 300 \text{ cm}^{-1}$  show a similar behavior with the excitation wavelengths  $\lambda = 632.8$  nm.

In proximity of the  $352\text{-cm}^{-1}$   $T_{2g}$  mode and the  $396\text{-cm}^{-1}$   $A_{1g}$  mode, the evolution of sidebands is observed at low temperatures. The  $T_{2g}$  mode at  $280 \text{ cm}^{-1}$  does not split (see Fig. 2). The temperature dependence of the peak frequencies shows a change of slope at  $T^*$ , and sidebands appear for  $T < T_c$ . The splittings themselves are rather small and of the order of 1–2% for the high-frequency modes. These observations are not compatible with a large reduction of symmetry and point to a preserved cubic symmetry.

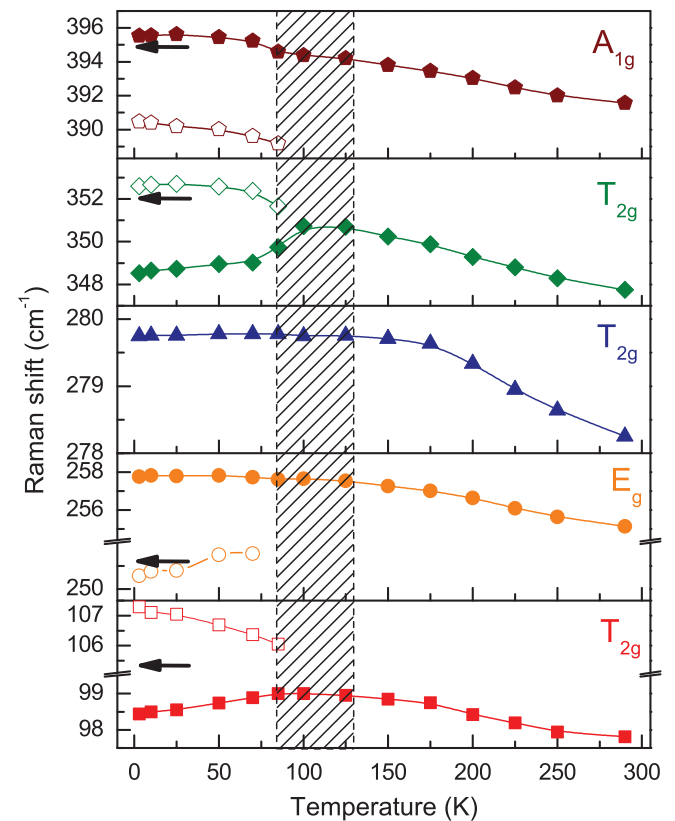


FIG. 2. (Color online) RS phonon frequency of  $\text{CdCr}_2\text{S}_4$  as a function of temperature. The fluctuation regime between  $T_c = 84.4$  K and  $T^* = 130$  K is marked by a dashed bar. Arrows mark the approximate frequency of LO phonons at  $T = 10$  K from earlier IR absorption experiments (Ref. 17).

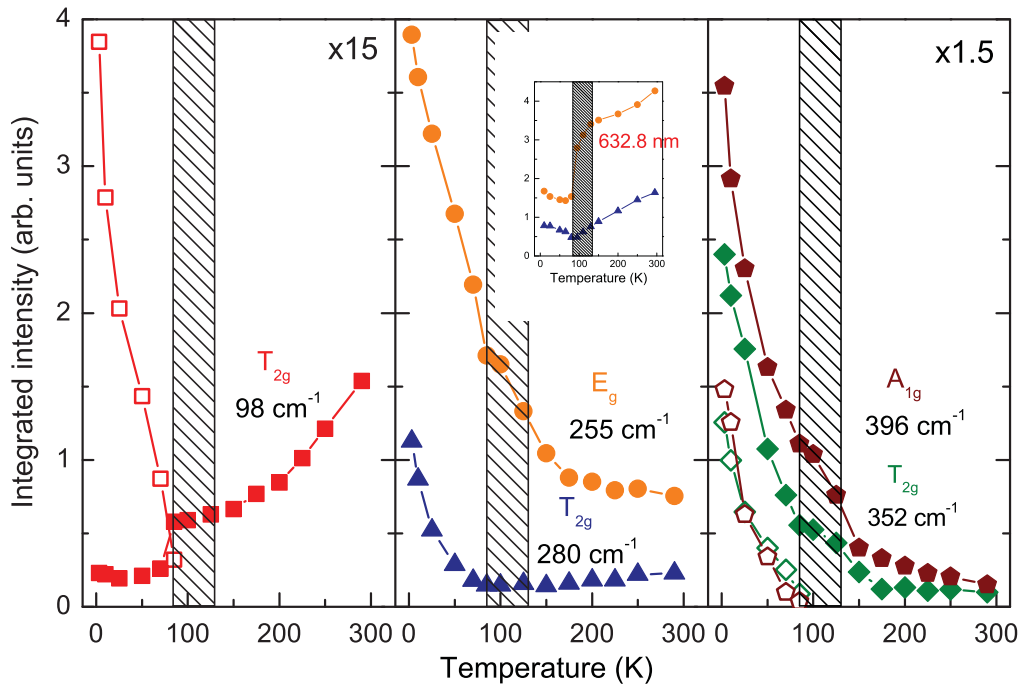


FIG. 3. (Color online) Integrated RS intensity of CdCr<sub>2</sub>S<sub>4</sub> as a function of temperature for the high-energy and the low-energy modes in the right panel (an exciting laser wavelength of  $\lambda = 532.1$  nm). The open symbols in the left and right panels correspond to the low-temperature modes at 106, 352, and 390 cm<sup>-1</sup>, respectively. The inset in the middle panel shows the results of the RS experiment with  $\lambda = 632.8$  nm.

In the same figure, the approximate frequencies of the low-temperature longitudinal optical (LO) modes from an earlier infrared absorption experiment are given by arrows.<sup>10,17</sup> It is obvious that the observed new modes are very close or coincide with these data within the accuracy of the earlier Kramers–Kronig analysis. For the 280-cm<sup>-1</sup>  $T_{2g}$  mode, no corresponding LO phonon exists,<sup>18</sup> and therefore no splitting can be detected. With a loss of inversion-only LO phonons, formerly IR active modes develop an RS cross section in backscattering geometry.

In Fig. 3 the phonon intensities of the high-temperature Raman active modes and additional modes are given. Both characteristic temperatures are evident in the data. Noteworthy is the large enhancement of the  $E_g$  mode and high-frequency  $T_{2g}$  and  $A_{1g}$  modes in the fluctuation regime between  $T_c$  and  $T^*$  at excitation under  $\lambda = 532.1$  nm. It leads to an overall increase by a factor 5 ( $E_g$ ) and 25 ( $T_{2g}$ ,  $A_{1g}$ ) to low temperatures. Interestingly, the intensity of the LO phonons increases with a similar slope down to lowest temperatures. The intensity of the 280-cm<sup>-1</sup> mode is nearly constant between  $T_c$  and  $T^*$  and enhances by a factor 8 to low temperatures. The intensity of the 98-cm<sup>-1</sup> mode drops in the whole temperature region with a sharp slope changing at  $T_c$ . In contrast, the intensity of the 280-cm<sup>-1</sup> and the 255-cm<sup>-1</sup> modes both drop by 70% in the high-temperature regime and recover only to about 1/3 of this intensity at low temperatures with an excitation at  $\lambda = 632.8$  nm.

The RS intensity of a phonon mode is proportional to the scattering volume and to the square of the electronic polarizability with respect to the displacement of the particular mode. A change of the surface conductivity may indeed obscure the intrinsic intensity evolution of phonon modes.

However, the scattering volume and optical penetration depth develop in parallel for all modes. Therefore, the observed very specific anomalies must at least be partly related to the local enhancement of electronic polarizability.

In Fig. 4 we show the temperature-dependent linewidths (full width at half maximum [FWHM]) of the phonon modes in CdCr<sub>2</sub>S<sub>4</sub>. The  $T$  dependencies of the FWHM of all modes show anomalies in the fluctuation regime and at the magnetic ordering temperature.

The left panel of Fig. 5 shows the low-energy  $T_{2g}$  and the related LO mode close to  $T_c$ . These modes demonstrate the largest splitting which facilitates their discrimination. With the onset of FM order, the  $T_{2g}$  mode is damped. The LO appears clearly at the magnetic transition. This behavior is different from the intensity gain that the high-energy  $T_{2g}$  mode shows for temperatures around  $T^*$ . At lowest temperature, the intensity of the sideband is comparable to the high-temperature intensity of the  $T_{2g}$  mode.

Previous investigations using circular, polarized light and optical pumping showed that resonance effects of the excitation wavelength with electronic states in CdCr<sub>2</sub>S<sub>4</sub> have to be considered.<sup>13</sup> These effects certainly complicate the interpretation of Raman scattering experiments. On the other side, they open up the opportunity to modify the local electronic properties of CdCr<sub>2</sub>S<sub>4</sub><sup>19</sup> by an internal photo effect and an electron transfer from the highly structured valence band of hybridized Cr  $t_{2g}$ -S 2p states to an unoccupied Cr  $e_g$ -Cd s high energy continuum.<sup>16</sup> The corresponding gap is  $\Delta = 1.6$ – $1.8$  eV.<sup>20</sup>

In the following, we will show evidence for a strong coupling of the phonon system to exactly these states. In Figs. 5(b) and 5(c) we compare RS with the previously used excitation

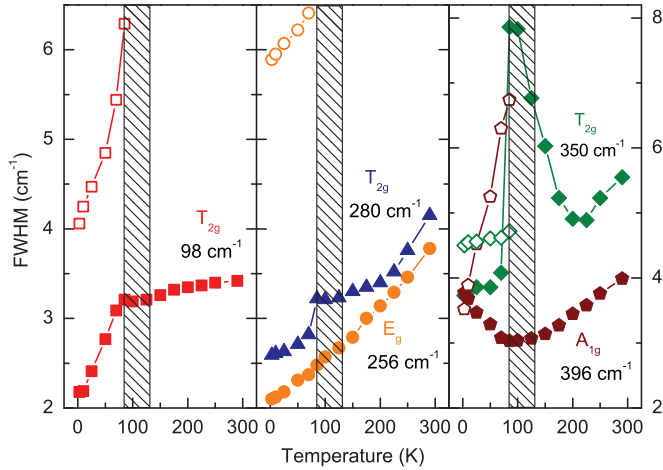


FIG. 4. (Color online) The Raman phonon widths as a function of temperature of  $\text{CdCr}_2\text{S}_4$ .

wavelength  $\Delta = 632.8 \text{ nm}$  (1.97 eV) and  $488 \text{ nm}$  (2.55 eV), respectively. The difference is rather drastic. A reversal of the effect of temperature on the RS spectra is evident, i.e. the intensity ratio of the  $T_{2g}$  to the LO phonon with  $488 \text{ nm}$  is close to that at  $T \approx T_c$  with  $632.8 \text{ nm}$ . This effect cannot be attributed to a modification of the selection rules similar to observations in resonance scattering on semiconductors<sup>21</sup> or a varying penetration depth as the intensities of both modes are affected. We attribute it to a local occupation of the antibonding  $\text{Cr } e_g\text{-Cd } s$  states within the conduction band. The high selectivity of the Raman intensity to the laser excitation energy reflects the difference in the lattice dynamics in which different phonons modulate different electronic bonds. Note that in accordance with the calculations by Lutz *et al.*<sup>15</sup> the vibration of  $95 \text{ cm}^{-1}$   $T_{2g}$  phonon mainly involves Cd ions displacements, while to the LO  $105 \text{ cm}^{-1}$  phonon, besides Cd vibrations, the Cr and S ions displacements also contribute.

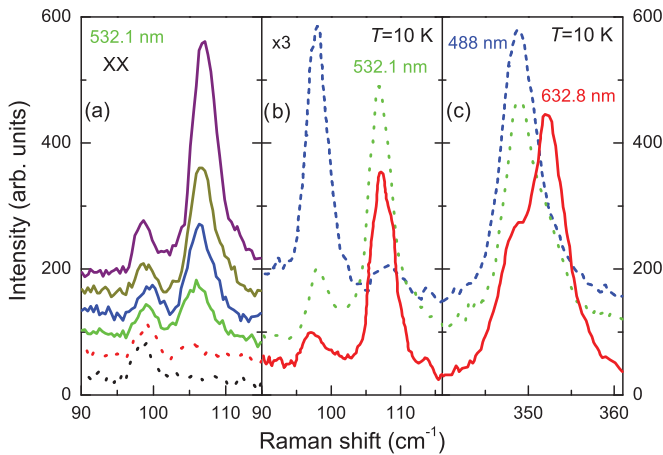


FIG. 5. (Color online) (a) Evolution of the low-frequency  $T_{2g}$  mode with an excitation wavelength of  $\lambda = 532.1 \text{ nm}$  at  $T = 10, 25, 65, 80, 95, 110 \text{ K}$ , from top to bottom. (b) and (c) RS experiments with  $\lambda = 488 \text{ nm}$  (top, dashed line),  $532.1 \text{ nm}$  (middle, dotted line), and  $632.8 \text{ nm}$  (bottom) at  $T = 10 \text{ K}$ . Curves have been shifted for clarity.

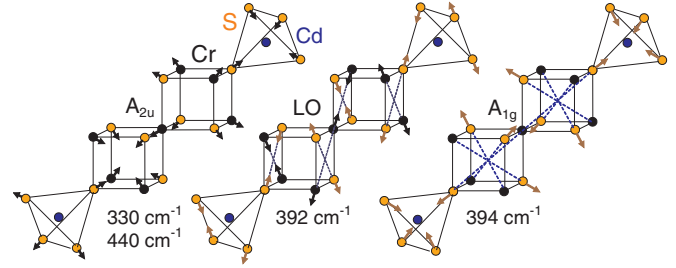


FIG. 6. (Color online) Displacement patterns and excitation energies of different modes that lead to a large modulation of the Cr-S hybridization (Refs. 15 and 23).

Understanding the anomalous magnetocapacitive behavior of  $\text{CdCr}_2\text{S}_4$  involves two issues. The first addresses the inconsistency between the high-temperature structure and the observed properties, i.e. global or local deviations from inversion symmetry. The second question concerns the interplay between local distortions and the spin polarization, i.e. the magnetocapacitive coupling mechanism. It must be outlined that a nonlinear relation between the corresponding fields and susceptibilities that is compatible with the observed phonon anomalies is a prerequisite but no proof of true magnetoelectricity.<sup>3,4</sup> In addition, spontaneous moments of proper magnitude should develop with decreasing temperatures.

With the present RS data, we give evidence that in  $\text{CdCr}_2\text{S}_4$  the inversion symmetry is lost, and the resulting low-temperature symmetry is reduced from  $Fd\bar{3}m$  to  $F\bar{4}3m$ . As shown in Fig. 6, a frozen  $A_{2u}$  mode corresponds to the long suggested Cr-off-centering.<sup>16</sup> The preserved cubic symmetry of  $F\bar{4}3m$  is the only way to describe the observed excitation spectrum.<sup>22</sup> Note that electric polarization is also not allowed by the symmetry of the  $F\bar{4}3m$  group. However, static  $A_{2u}$ -type distortions provide magnetoelectric coupling between magnetic and polar degrees of freedom. This low-temperature structure allows invariants of the free energy  $F \propto M_x M_y P_z + M_y M_z P_x + M_x M_z P_y$  with an electric polarization  $P$  with some direction to a net magnetic moment  $M$ .<sup>22</sup> This kind of invariant was prohibited in the earlier accepted  $Fd\bar{3}m$  space group.

Cubic symmetry is conserved by  $A_{2u}$  with Cr and S static displacements, two nonequivalent Cr sites and two alternating S-Cd bond lengths. In the new symmetry, the atom-occupied sites are 4a-Cd(1), 4d-Cd(2), 16e-Cr, 16e-S(1), 16e-S(2). The additional modes are a result of the related  $A_{2u}$  displacement that evolves into a long-range distortion for  $T < T_c$ . The number of Raman allowed modes are  $\Gamma = 3A_1 + 3E + 7T_2$ . Besides the previously observed  $1A_{1g}(A_1)$ ,  $1E_g(E)$ , and  $3T_{2g}(T_2)$ , this number is enlarged by the former  $2A_{2u}(A_1)$  and  $2E_u(E)$  silent modes related to S and Cr displacements as well by  $4T_{1u}(T_2)$  of far-infrared polar modes. Calculations give  $A_{2u}$  modes<sup>23</sup> at  $331$  and  $422 \text{ cm}^{-1}$  and  $E_u$  modes  $214$  and  $357 \text{ cm}^{-1}$ . Those calculations have been done on the basis of semi-empirical models. Nevertheless, below  $T_c$  we observe in the respective energy range additional lines at  $238, 371,$  and  $378 \text{ cm}^{-1}$ , which could be attributed to the previously silent modes.



In addition to the single-phonon scattering, some lines in our Raman spectra of  $\text{CdCr}_2\text{S}_4$  can be interpreted as a multiple-order scattering that is a fingerprint of lattice anharmonicity. Note that assuming a second-order phase transition from  $Fd\bar{3}m$  to  $F43m$  in the high-temperature phase, one of the  $A_{2u}$  modes must demonstrate a soft-mode behavior. However, this cannot be detected by far-infrared or Raman studies. In its turn, under the approaching of  $T_c$  from low-temperature phase, one of the  $A_1$  modes should be a soft mode and can be seen in Raman spectra.

The intensity-polarizability enhancements of all high-frequency modes are strong evidence for pronounced nonlinearities of the coupled electronic-lattice systems. The intensity of these modes and the LO sidebands is still increasing in the temperature range where the macroscopic magnetization does not change very much.<sup>5</sup> In Fig. 6, we sketch displacements with enhanced polarizability, and it is evident that all modes effectively modulate the hybridization of the Cr  $t_{2g}$ -S 2p states by a simultaneous stretching–squeezing of the S-Cd and S-Cr bonds, respectively.<sup>12,15</sup> In contrast, the intermediate frequency modes show an antiphase stretching on the opposite sides of the S-Cr cube. Depending on the relative amplitude of the Cr and S displacements, such a motion can cancel the contribution of all S-Cr bonds to the dielectric response as well as to the RS response. This is in our opinion the origin of the minimum observed in the intensity of, for example, the  $255\text{-cm}^{-1}$  mode with  $632.8\text{ nm}$  excitation and for temperatures below  $T_c$ . The displacements sketched in Fig. 6 could also be interpreted as a Cr-Cr dimer formation. Such structural correlations lead to large energy gains on frustrated topologies, i.e. it leads to the spin gap formation in  $\text{MgTi}_2\text{O}_4$ <sup>24</sup> and  $\text{CuIr}_2\text{S}_4$ .<sup>25</sup> For  $\text{CdCr}_2\text{S}_4$  the hybridized states, including some nonstoichiometry, provide a finite but small density of states at the Fermi energy.<sup>26</sup>

The presently discussed magnetoelectrics provide a rather complex picture of possible mechanisms for large cross susceptibilities.<sup>1</sup> Systematic investigations of the phonon frequencies and the magnetic ground state of different chromium spinels show that  $\text{CdCr}_2\text{S}_4$  is close to a bond-frustrated phase with enhanced spin-electron-phonon coupling.<sup>10</sup> For some rare earth perovskites, such as  $\text{RCrO}_3$  ( $R = \text{La, Y, Lu}$ ), similar conclusions have been drawn as well as the observation of multiferroicity attributed to certain modulations of the Cr-O-Cr bond angle and length.<sup>27</sup> To describe the tendency for spontaneous polarizations and off-centering,<sup>28,29</sup> the concept of a second-order Jahn–Teller effect has been

used. This effect is based on the hybridization of nearly degenerate electronic states of appropriate symmetry<sup>3,4</sup> that overcompensates the cost of Coulomb energy due to the distortions of occupied 3d electron systems. In multiferroic  $\text{BiFeO}_3$ , the off-centering of Bi is a result of a hybridization of both the Bi  $6s^2$  and unoccupied  $6p^0$  states with O 2p orbitals leading to a highly polarizable lone pair on one side of the Bi ion.<sup>30</sup> Weaker displacements and anomalies of the Raman scattering intensity have been observed for the case of  $\text{Cd}^{2+}$  ions in sulfur environments, e.g. in  $\text{CdPS}_3$ .<sup>31</sup> We therefore attribute the enhanced local polarizabilities caused by diagonal S displacements in  $\text{CdCr}_2\text{S}_4$  to hybridization effects of moderately correlated Cd and S states.<sup>16</sup> This also agrees with recent observations of the effect of electric fields on electric transport.<sup>32</sup>

The lattice degrees of freedom provide another peculiarity. The energy splitting between polar and nonpolar modes in  $\text{CdCr}_2\text{S}_4$  is extremely small compared to other energy scales of the system. Evidently, it reflects some internal degeneracy of the lattice subsystem. This accidental degeneracy can easily be removed by third- or higher-order anharmonicity with a negligible restoring force. Moreover, one can expect that the respective distortion of the  $Fd\bar{3}m$  structure being dynamic at high temperatures becomes static at lower ones. More direct evidence, however, must come from high-resolution diffraction experiments that should indicate electronic redistribution within the  $\text{S}_6$  octahedra or a large atomic displacement parameter of  $\text{Cd}^{2+}$  in the fluctuation regime.

#### IV. CONCLUSIONS

Summarizing, Raman scattering experiments on stoichiometric single crystals of  $\text{CdCr}_2\text{S}_4$  prepared by Br transport reactions show pronounced phonon anomalies that are evidence for a symmetry reduction and Cr off-centering in the cubic unit cell. The resulting enhanced electronic polarizability of displacements that modulate the Cr-S distance is proposed as a microscopic mechanism for the observed large magnetocapacitive effects.

#### ACKNOWLEDGMENTS

We acknowledge support by DFG and FRSF of Ukraine Grant No. F29.1/014. K.Y.C. acknowledges support by the Alexander-von-Humboldt Foundation and Korea NRF Grant No. 2009-0093817.

<sup>1</sup>T. Kimura, T. Goto, H. Shintani, K. Ishizaka, T. Arima, and Y. Tokura, *Nature (London)* **426**, 55 (2003); N. Hur, S. Park, P. A. Sharma, J. S. Ahn, S. Guha, and S.-W. Cheong, *ibid.* **429**, 392 (2004); Th. Lottermoser, Th. Lonkai, U. Amann, D. Hohlwein, J. Ihringer, and M. Fiebig, *ibid.* **430**, 541 (2004); T. Goto, T. Kimura, G. Lawes, A. P. Ramirez, and Y. Tokura, *Phys. Rev. Lett.* **92**, 257201 (2004); N. Hur, S. Park, P. A. Sharma, S. Guha, and S. W. Cheong, *ibid.* **93**, 107207 (2004); B. B. Van Aken, T. T. M. Palstra, A. Filippetti, N. A. Spaldin, *Nat. Mater.* **3**, 164 (2004); Y. Tokura and Sh. Seki, *Adv. Mater.* **22**, 1554 (2010).

<sup>2</sup>H. Zheng *et al.*, *Science* **303**, 661 (2004); I. Levin *et al.*, *Adv. Matter* **18**, 2044 (2006); R. Ramesh and N. A. Spaldin, *Nat. Mater.* **6**, 21 (2007).

<sup>3</sup>M. Fiebig, *J. Phys. D: Appl. Phys.* **38**, R123 (2005).

<sup>4</sup>N. A. Spaldin and M. Fiebig, *Science* **309**, 391 (2005); *Curr. Opin. Solid State Mater. Sci.* **9**, 128 (2005); N. A. Hill, *J. Phys. Chem. B* **104**, 6694 (2000).

<sup>5</sup>J. Hemberger, P. Lunkenheimer, R. Fichtl, H.-A. Krug von Nidda, V. Tsurkan, and A. Loidl, *Nature (London)* **434**, 364 (2005).

- <sup>6</sup>H. Gobel, *J. Magn.Magn. Mater.* **3**, 143 (1976).
- <sup>7</sup>P. Lunkenheimer, R. Fichtl, J. Hemberger, V. Tsurkan, and A. Loidl, *Phys. Rev. B* **72**, 060103(R) (2005).
- <sup>8</sup>E. Dagotto, *Phase Separation and Colossal Magnetoresistance*, (Springer, Berlin) 2002.
- <sup>9</sup>G. Catalan and J. F. Scott, *Nature* **448**, E4 (2007); J. Hemberger, P. Lunkenheimer, R. Fichtl, H.-A. Krug von Nidda, V. Tsurkan, and Loidl, *ibid.* **448**, E5 (2007), and references therein.
- <sup>10</sup>T. Rudolf, C. Kant, F. Mayr, J. Hemberger, V. Tsurkan, and A. Loidl, *Phys. Rev. B* **76**, 174307 (2007), and references therein.
- <sup>11</sup>H. Schmid and E. Ascher, *J. Phys. C* **7**, 2697 (1974), and references therein.
- <sup>12</sup>E. F. Steigmeier and G. Harbecke, *Phys. Condens. Matter* **12**, 1 (1970).
- <sup>13</sup>N. Koshizuka, S. Ushioda, and T. Tsushima, *Phys. Rev. B* **21**, 1316 (1980), and references therein; N. Sanford, R. W. Davies, A. Lempicki, W. J. Miniscalco, and S. J. Nettel, *Phys. Rev. Lett.* **50**, 1803 (1983).
- <sup>14</sup>Intensity anomalies in Ref. 12 are spurious due to a strongly temperature dependent reference mode. The later study in Ref. 13 did not have sufficient resolution to allow a separate observation of splitted modes.
- <sup>15</sup>H. D. Lutz, J. Himmrich, and H. Haeuseler, *Z. Naturforsch. A* **45**, 893 (1990).
- <sup>16</sup>C. J. Fennie and K. M. Rabe, *Phys. Rev. B* **72**, 214123 (2005).
- <sup>17</sup>K. Wakamura and T. Arai, *J. Appl. Phys.* **63**, 5824 (1988).
- <sup>18</sup>IR modes at  $T = 10$  K have been reported in Ref. 17 as LO modes at 105.2, 251.2, 352.1, 395.0 and as TO modes at 101.8, 248.8, 323.5 and 379.0  $\text{cm}^{-1}$ . Almost the same values have been obtained in Ref. 10 under extrapolation to  $T = 0$  K.
- <sup>19</sup>G. Güntherodt and R. Zeyher, in *Light Scattering in Solids IV*, edited by G. Güntherodt and M. Cardona (Springer, Berlin, 1984), and references therein.
- <sup>20</sup>W. J. Miniscalco, B. C. McCollum, N. G. Stoffel, and G. Margaritondo, *Phys. Rev. B* **25**, 2947 (1982).
- <sup>21</sup>Fingerprints are higher order multiphonon scattering, broadening of modes and fluorescence effects, see W. Kauschke, N. Mestres, and M. Cardona, *Phys. Rev. B* **36**, 7469 (1987).
- <sup>22</sup>Implications of  $F\bar{4}3m$  for spinel compounds can be found in Ref. 11.
- <sup>23</sup>J. Zwinscher and H. D. Lutz, *J. Solid State Chem.* **118**, 43 (1995).
- <sup>24</sup>M. Isobe and Yu. Ueda, *J. Phys. Soc. Jpn.* **71**, 1848 (2002).
- <sup>25</sup>P. G. Radaelli, Y. Horibe, M. J. Gutmann, H. Ishibashi, C. H. Chen, R. M. Ibberson, Y. Koyama, Yew-San Hor, Valery Kiryukhin, and S.-W. Cheong, *Nature* **416**, 155 (2002).
- <sup>26</sup>N. Shanthi, P. Mahadevan, and D. D. Sarma, *J. Solid State Chem.* **155**, 198 (2000).
- <sup>27</sup>N. Ray and U. V. Waghmare, *Phys. Rev. B* **77**, 134112 (2008).
- <sup>28</sup>R. G. Pearson, *Proc. Nat. Acad. Sci. USA* **72**, 2104 (1975).
- <sup>29</sup>J. K. Burdett and O. Eisenstein, *Inorg. Chem.* **31**, 1758 (1992).
- <sup>30</sup>J. B. Neaton, C. Ederer, U. V. Waghmare, N. A. Spaldin, and K. M. Rabe, *Phys. Rev. B* **71**, 014113 (2005).
- <sup>31</sup>F. Boucher, M. Evain, and R. Brec, *Acta Crystallogr. Sect. B* **51**, 952 (1995).
- <sup>32</sup>C. P. Sun, C. C. Lin, J. L. Her, C. J. Ho, S. Taran, H. Berger, B. K. Chaudhuri, and H. D. Yang, *Appl. Phys. Lett.* **96**, 122109 (2010); C. P. Sun, C. L. Huang, C. C. Lin, J. L. Her, C. J. Ho, J.-Y. Lin, H. Berger, and H. D. Yang, *Phys. Rev. B* **79**, 214116 (2009).